

Study on Redundancy in Robot Kinematic Parameter Identification

YUE ZHANG¹, JIAWEN GUO², AND XUEYAN LI¹

¹School of Space Science and Technology, Xidian University, Xi'an 710126, China

²School of Astronautics, Harbin Institute of Technology, Harbin 150001, China

Corresponding author: Yue Zhang (zhangyue@xidian.edu.cn)

This work was supported in part by the Science and Technology on Space Intelligent Control Laboratory under Grant HTKJ2019KL502016, and in part by the China Scholarship Council (CSC) under Grant 201806120093.

ABSTRACT The robot kinematic error model may include redundant parameters, which require removal prior to the identification of kinematic parameters to ensure the accuracy and stability of such. Traditionally, the redundant parameters are determined by the numerical analysis. This paper presents an analytical method to determine the identifiable kinematic parameters for serial-robot calibration under various identification conditions. Among various kinematic models of robots, the DH (Denavit-Hartenberg) model is the most commonly used, so the analysis of redundant parameters is based on the DH error model. The correlation between the columns of the Jacobian matrix is analyzed by theoretical methods, resulting in the linear relationship between these columns. The redundant error parameters and the linear independent parameters after removing redundancies from robots with different measurement conditions and different configurations are clearly given. Thus, the redundant parameters can be easily determined based on the values of kinematic parameters, which facilitates the determination of the non-redundant kinematic calibration model. In addition, the physical meanings of redundant parameters are also elaborated, which can reveal the inherent principle of the error parameters' linear correlation. Finally, the parameter identification simulation experiment shows that the identification results, after removing the redundant parameters, all converge to the true values when the random noise is not considered, which verifies the correctness of the parameter redundancy analysis results. In the case of considering random noise, the non-redundant parameter identification has better convergence than the full parameter identification. This study can provide theoretical and application references for robot kinematic calibration.

INDEX TERMS Robot, kinematic parameters, identification, redundant, Jacobian matrix, calibration.

I. INTRODUCTION

High-end positioning accuracy is required for space robots capturing space targets in orbit and installing equipment, for assembly robots on production lines, and for robots for medical services. Presently, the repeating positioning accuracy of the industrial robots is high, but the absolute accuracy is still not high [1], [2]. Robot machining and assembly errors, joint clearance, and arm deformation can cause robot end errors. The geometric errors generated during the machining and assembly of the robot components are the most important factors affecting the robot end accuracy. This part of the error accounts for 90% of all the error sources [1]. Therefore, to improve the absolute accuracy of a robot, it is necessary

to identify the kinematic parameter error of the robot and compensate for it [3]–[5].

A robot's kinematic parameter identification needs to obtain its end pose data through experimental measurement and then, acquire the error of the kinematic parameters based on the specific identification model and algorithm. However, because some kinematic parameters have the same effects on the end pose, it is impossible to distinguish the size of each kinematic parameter error based on the end error; namely, there are redundant parameters in the identification model [6]–[8]. Because the noise in the experimental measurement is unavoidable, the existence of redundant parameters adversely affects the accuracy and stability of the kinematic parameter identification of the robot, thus influencing the optimization effect of the end precision of the robot. Therefore, it is necessary to remove the redundant parameters before identification [9]–[12].

The associate editor coordinating the review of this manuscript and approving it for publication was Hui Xie¹.

If there exist redundant parameters, only the linear combination of these kinematic parameters can be identified. The redundant parameters are determined by the kinematic model of the robot, regardless of which identification algorithm is used. Up till now, various kinematic models of robots have been proposed, such as DH (Denavit-Hartenberg) model [13]–[17], CPC (Complete and Parametrically Continuous) model [18], [19], S model [20]–[22], zero reference model [6], [23] and POE (Product of Exponentials) model [11], [24]. On the research of redundant parameters, Everett *et al.* [25], [26] analyzed the maximum number of independent kinematic parameters of robots with rotary and translational joints for the first time, and demonstrated how to model any manipulator so that a minimum size Jacobian is used, thus reducing the computation required for calibration. However, the redundant parameters for robots with different configurations cannot be determined. Zhuang *et al.* [18], [19] proposed the CPC model to describe the motion of robots, each joint contains six kinematic parameters, among them three parameters are used to describe the direction of joint axis, while the others are used to describe the position relationship between the adjacent joints. Although some of these parameters are redundant parameters, they can be systematically eliminated in the process of constructing the error models. Gupta [23] established the zero reference model, in which the direction and position of each joint axis are described relative to a zero reference configuration, and there exist redundant parameters in the kinematic error model. For specific cases, the redundant parameters may be eliminated by ignoring the revolute and translation error in the particular direction, but the general validation is absent now [27]. Meggiolaro and Dubowsky [28] analyzed the redundancy of generalized errors, in which the analytical expressions of the redundant parameters are presented. On the basis of these expressions, the redundant parameters can be eliminated from the error model. In order to analyze the redundant parameters in POE model, Chen *et al.* [29], [30] constructed an orthogonal partitioning matrix in a straightforward way and then the redundant error parameters can be determined and eliminated from the POE model.

As analyzing the linear correlation columns of the identification matrix is relatively complicated, most of the prior art on redundant parameters focused on the analysis for specific cases, which especially lacked the versatility analysis and verification for DH parameters. In this paper, modeling and parameter redundancy analyses are carried out accordingly.

This paper first establishes the robot kinematic error model for parameter identification. On this basis, the paper analyzes the redundancy of the parameters, resulting in the redundant parameters and linear independent parameters under different conditions. The physical meanings have also been explained. Finally, simulation experiments verify the redundancy analysis results. There are two main innovations in this work. First, this paper analyzes the redundant DH parameters of any serial robot under different measurement conditions and geometric configurations, with a demonstrated universality.

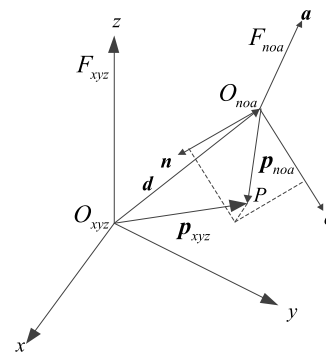


FIGURE 1. The position vectors of point P in the two coordinate systems.

The resulted redundant parameters and the linear independent parameter list can be used to quickly determine the redundant parameters of the robot and to perform non-redundant parameter identification. Second, this paper explains the physical meanings of different redundant DH parameters and reveals the inherent principle of the error parameters’ linear correlation.

II. ROBOT KINEMATIC ERROR MODEL

A. KINEMATIC DESCRIPTION

Robot kinematics modeling refers to calculating the end position and attitude of a robot under the condition that the robot joint variables and geometric parameters are known. First, the homogeneous coordinate transformation between the two coordinate systems is discussed, and then, the kinematic model of the robot is given based on the DH parameters.

Figure 1 shows the position vectors of point P in two coordinate systems, where the coordinate system F_{xyz} is the reference coordinate system, and F_{noa} is the relative coordinate system. The unit vectors of the coordinate system F_{noa} in the three directions are n, o, a , respectively, which are indicated in the reference coordinate system F_{xyz} . The position vectors of an arbitrary point P in the two coordinate systems are given in the figure.

The homogeneous transformation matrix is defined as follows [31]:

$${}^{xyz}A_{noa} = \begin{bmatrix} n_x & o_x & a_x & d_x \\ n_y & o_y & a_y & d_y \\ n_z & o_z & a_z & d_z \\ 0 & 0 & 0 & 1 \end{bmatrix} \quad (1)$$

The homogeneous transformation matrix in the above equation consists of four vectors, including three direction vectors and one position vector. The homogeneous transformation matrix can simultaneously transform the position and attitude between the two coordinate systems. To realize the linear transformation of the position vectors between the different coordinate systems, it is necessary to represent the position of point P as the 4×1 vector.

$$p = [p_x \quad p_y \quad p_z \quad 1]^T \quad (2)$$

At this time, the relationship of the position vectors of Point P in the two coordinate systems can be expressed as follows:

$$p_{xyz} = {}^{xyz}A_{noa} p_{noa} \quad (3)$$

In this paper, the DH method, which was proposed by Denavit and Hartenberg [13] is used to model the kinematic parameters of the robots. There are four DH parameters for each joint, namely the joint distance d_i , joint angle θ_i , rod length a_i , and rod twist angle α_i . For a rotating joint, d_i , a_i , and α_i are constant values, whereas θ_i changes as the joint rotates. The specific definitions of each parameter are as follows:

- (1) Joint distance d_i : The distance from axis X_{i-1} to axis X_i . The direction towards axis Z_{i-1} is defined as positive;
- (2) Joint angle θ_i : The angle from axis X_{i-1} to axis X_i . The positive rotation around axis Z_{i-1} is defined as positive;
- (3) Rod length a_i : the distance from axis Z_{i-1} to axis Z_i . The direction towards axis X_i is positive; and
- (4) Rod twist angle α_i : The angle from axis Z_{i-1} to axis Z_i . The positive rotation around axis X_i is defined as positive.

The homogeneous transformation matrix of coordinate system F_i corresponding to the coordinate system F_{i-1} is the product of four basic transformations:

$${}^{i-1}A_i = A_{Trans}(0, 0, d_i)A_{Rot}(z_i, \theta_i)A_{Trans}(a_i, 0, 0)A_{Rot}(x_i, \alpha_i) \\ = \begin{bmatrix} \cos \theta_i & -\cos \alpha_i \sin \theta_i & \sin \alpha_i \sin \theta_i & a_i \cos \theta_i \\ \sin \theta_i & \cos \alpha_i \cos \theta_i & -\sin \alpha_i \cos \theta_i & a_i \sin \theta_i \\ 0 & \sin \alpha_i & \cos \alpha_i & d_i \\ 0 & 0 & 0 & 1 \end{bmatrix} \quad (4)$$

Here, A_{Trans} and A_{Rot} are the homogeneous transformation matrices of the translation and rotation operation for the coordinate system. For the robot with N degrees of freedom, the homogeneous coordinate transformation matrix from coordinate system F_N to F_0 is

$${}^0A_N = {}^0A_1 {}^1A_2 \dots {}^{N-2}A_{N-1} {}^{N-1}A_N \quad (5)$$

B. ERROR MODEL DERIVATION

To identify the kinematic parameters of the robot, it is necessary to obtain the kinematic error model of the robot—specifically, the relationship between the pose error of the end actuator and the slight deviation of the kinematic parameters. The relationship between the two is determined by the parameter identification Jacobian matrix.

1) ERROR MODEL BETWEEN ADJACENT JOINT COORDINATE SYSTEMS

First, the error model between the adjacent two joint coordinate systems is given; namely, the joint pose error are calculated according to the joint DH parameter error. Assuming the DH parameter error of joint i is $\Delta X_i = [\Delta \theta_i \ \Delta \alpha_i \ \Delta d_i \ \Delta a_i]^T$, the robot joint pose error is $D_i = [dx_i \ dy_i \ dz_i \ \delta x_i \ \delta y_i \ \delta z_i]^T$, where dx_i , dy_i , and dz_i are the infinitesimal translational displacement, δx_i , δy_i , and δz_i are the infinitesimal rotation angles around axes x_i , y_i , and z_i , respectively.

The variation of the homogeneous transformation matrix caused by the robot DH parameter error dA_i can be expressed as [32]

$$dA_i = \frac{\partial A_i}{\partial \theta_i} \Delta \theta_i + \frac{\partial A_i}{\partial \alpha_i} \Delta \alpha_i + \frac{\partial A_i}{\partial d_i} \Delta d_i + \frac{\partial A_i}{\partial a_i} \Delta a_i \quad (6)$$

which can be simplified as follows (7), as shown at the bottom of the next page.

The variation of the homogeneous transformation matrix caused by the robot joint pose error dA_i satisfies the following:

$$A_i + dA_i \\ = A_i(A_{Trans}(dx_i, dy_i, dz_i)A_{Rot}(x_i, \delta x_i)A_{Rot}(y_i, \delta y_i) \\ \times A_{Rot}(z_i, \delta z_i)) \\ = A_i \delta A_i \quad (8)$$

Considering D_i is a tiny item, the second-order small amount can be ignored in the calculation.

$$\delta A_i = \begin{bmatrix} 1 & -\delta z_i & \delta y_i & dx_i \\ \delta z_i & 1 & -\delta x_i & dy_i \\ -\delta y_i & \delta x_i & 1 & dz_i \\ 0 & 0 & 0 & 1 \end{bmatrix} \quad (9)$$

The relationship between the joint pose error and the DH parameter error can be obtained by combining equations (7)–(9):

$$\begin{bmatrix} dx_i \\ dy_i \\ dz_i \\ \delta x_i \\ \delta y_i \\ \delta z_i \end{bmatrix} = \begin{bmatrix} 0 & 0 & 0 & 1 \\ a_i \cos \alpha_i & 0 & \sin \alpha_i & 0 \\ -a_i \sin \alpha_i & 0 & \cos \alpha_i & 0 \\ 0 & 1 & 0 & 0 \\ \sin \alpha_i & 0 & 0 & 0 \\ \cos \alpha_i & 0 & 0 & 0 \end{bmatrix} \begin{bmatrix} \Delta \theta_i \\ \Delta \alpha_i \\ \Delta d_i \\ \Delta a_i \end{bmatrix} \quad (10)$$

which can be simplified as follows:

$$D_i = L_i \Delta X_i \quad (11)$$

2) ERROR MODEL OF END COORDINATE SYSTEM

For the robot with N degrees of freedom, the error model of the robot end coordinate system can be obtained from the error model between the two joint coordinate systems obtained in the previous section. There are $4N$ unknown error parameters in the robotic kinematic error models. Considering the small parameter error, the high-order small amount can be ignored in the calculation. At this time, the robot end pose error is a linear superposition of the end pose error caused by the DH parameter error of each joint:

$${}^E D = \sum_{i=1}^N {}^E D_i = \sum_{i=1}^N {}^E F_i \cdot D_i \quad (12)$$

Here, ${}^E D_i$ is the robot end pose error when only the parameter error of the joint i is considered. The superscript E indicates that they are all defined in the end coordinate system. Moreover, ${}^E F_i$ is the transformation matrix for the pose errors from the joint i coordinate system to the end coordinate

system, which can be expressed as the continuous product of the transformation matrix for the adjacent joint coordinate systems:

$${}^E_i F = \begin{cases} F^N \cdot F^{N-1} \dots F^{i+1} & i \leq N - 1 \\ I & i = N \end{cases} \quad (13)$$

Here, F^i indicates the pose error transformation matrix from the coordinate system of joint $i-1$ to that of joint i , expressed as follows (14), as shown at the bottom of the next page.

Substituting equation (11) into equation (12), and then, the relationship between the robot end pose error and the DH parameter error of each joint can be obtained as follows:

$${}^E D = \sum_{i=1}^N {}^E_i F L_i \Delta X_i \quad (15)$$

This can be written into a matrix form as included below:

$${}^E D = \begin{bmatrix} {}^E_1 F L_1 & {}^E_2 F L_2 & \dots & {}^E_{N-1} F L_{N-1} & {}^E_N F L_N \end{bmatrix} \times \begin{bmatrix} \Delta X_1 \\ \Delta X_2 \\ \vdots \\ \Delta X_{N-1} \\ \Delta X_N \end{bmatrix} = J \Delta X \quad (16)$$

The above equation is the error model of the robot end coordinate system, where J is the Jacobian matrix for the parameters identification, and ΔX is the DH parameter error of all joints.

The robot end coordinate system error model includes two parts: the end position error model and the end attitude error model. Therefore, equation (16) can also be written as follows:

$$\begin{bmatrix} E d \\ E \delta \end{bmatrix} = \begin{bmatrix} d J \\ \delta J \end{bmatrix} \Delta X \quad (17)$$

III. DH PARAMETER REDUNDANCY ANALYSIS

In the actual parameter calibration experiment, noise is inevitably accompanied when measuring the end position of the robot and the angle value of each joint, resulting in the deviations in the identification results [33], [34]. The impacts of random noise on the identification results are closely related to the identification model. If there are redundant parameters in the identification model, the identification Jacobian matrix J is rank deficit. According to the definition of the matrix condition number, the condition number of matrix J will be infinite, and the existence of noise can affect the accuracy of parameter identification to a large extent,

thus affecting the optimization effect of the end precision of the robot. Therefore, the parameter redundancy needs to be analyzed before performing parameter identification, and then, the redundant parameters should be removed from the identification model to obtain linear independent error parameters. This ensures the accuracy and stability of parameter identification.

A. CORRELATION ANALYSIS

If there are redundant parameters in the parameter identification model, the identification Jacobian matrix J must not be the full column rank. Therefore, some sub-columns of the Jacobian matrix are linearly correlated. Assuming the number of redundant parameters is r , then the highest rank of the matrix is $4N - r$ —meaning, the Jacobian matrix has a group of r linearly correlated sub-columns.

According to the equation (16), the parameter identification Jacobian matrix is

$$J = \begin{bmatrix} {}^E_1 F L_1 & {}^E_2 F L_2 & \dots & {}^E_{N-1} F L_{N-1} & {}^E_N F L_N \end{bmatrix} \quad (18)$$

For the serial robots, the linear combination of all the sub-columns of the Jacobian matrix can be represented by the linear combination of the two adjacent joint coordinate systems. The parameter identification Jacobian matrix of the joint i and joint $i - 1$ are as follows:

$$J_{i-1} = F^N \cdot F^{N-1} \dots F^{i+1} \cdot F^i L_{i-1} = {}^E_i F \cdot F^i L_{i-1} = {}^E_i F \cdot J_{i-1}^* \quad (19)$$

$$J_i = F^N \cdot F^{N-1} \dots F^{i+1} \cdot L_i = {}^E_i F \cdot L_i = {}^E_i F \cdot J_i^* \quad (20)$$

For the adjacent, two joint coordinate systems, the following linear combination is considered to exist:

$$k_1 J_{\theta_{i-1}} + k_2 J_{\alpha_{i-1}} + k_3 J_{d_{i-1}} + k_4 J_{a_{i-1}} = k_5 J_{\theta_i} + k_6 J_{\alpha_i} + k_7 J_{d_i} + k_8 J_{a_i} \quad (21)$$

Here, $k_1 \dots k_8$ are arbitrary constants. If both of them are zero, then $[J_{i-1} \ J_i]$ is a full rank matrix, and there is no redundant parameter.

Because there is no parameter correlated to joints i and $i - 1$ in ${}^E_i F$, matrices $[J_{i-1} \ J_i]$ and $[J_{i-1}^* \ J_i^*]$ have same linear combinations, according to equation (19) and equation (20). Therefore, it is not necessary to calculate the specific expression of the Jacobian matrix. The linear correlation columns of the Jacobian matrix can be obtained through J_{i-1}^* and J_i^* .

$$dA_i = A_i \begin{bmatrix} 0 & -\cos \alpha_i \Delta \theta_i & \sin \alpha_i \Delta \theta_i & \Delta a_i \\ \cos \alpha_i \Delta \theta_i & 0 & -\Delta \alpha_i & a_i \cos \alpha_i \Delta \theta_i + \sin \alpha_i \Delta d_i \\ -\sin \alpha_i \Delta \theta_i & \Delta \alpha_i & 0 & -a_i \sin \alpha_i \Delta \theta_i + \cos \alpha_i \Delta d_i \\ 0 & 0 & 0 & 0 \end{bmatrix} \quad (7)$$

B. LINEARLY CORRELATED COLUMNS OF JACOBIAN MATRIX

In this section, the redundant error parameters of the robot are obtained by analyzing the linearly correlated columns of the Jacobian matrix with different identification conditions (such as measuring the end pose or only measuring the end position) and different configurations.

1) MEASURING THE END POSE

Matrices J_{i-1}^* and J_i^* can be obtained with the following equation:

$$J_{i-1}^* = F^i L_{i-1}, \quad J_i^* = L_i \quad (22)$$

According to equations (21) and (22) as given in (23), as shown at the bottom of the next page.

For a joint-rotating robot, θ_i is the variable. The above equation holds true in the cases included below.

1. If $\sin \alpha_{i-1} \neq 0$, i.e., $\alpha_{i-1} \neq 0$ and $\alpha_{i-1} \neq 180^\circ$, then

$$\begin{aligned} k_1 = k_2 = k_6 = 0, \quad k_5 = 0 \\ k_3 = k_4 = k_8 = 0, \quad k_7 = 0 \end{aligned} \quad (24)$$

There is no linearly correlated column in the Jacobian matrix at this time, so there are no redundant parameters.

2. If $\sin \alpha_{i-1} = 0$, i.e., $\alpha_{i-1} = 0$ and $\alpha_{i-1} = 180^\circ$, then

$$\begin{aligned} k_2 = k_6 = 0, \quad k_1 = \pm k_5 \\ \pm k_1 \sin \theta_i a_{i-1} + k_4 \cos \theta_i = k_8 \end{aligned} \quad (25)$$

Now, we calculate $k_1 \cdots k_8$ with different values of a_{i-1} to obtain linearly correlated columns in the Jacobian matrix.

a) If $a_{i-1} \neq 0$, then

$$\begin{aligned} k_2 = k_6 = 0, \quad k_1 = k_5 = k_4 = k_8 = 0 \\ k_3 = \pm k_7 \end{aligned} \quad (26)$$

If we substitute the above equation into the equation (21), it results in the following linear relationship existing in the Jacobian matrix:

$$J_{d_{i-1}} = \pm J_{d_i} \quad (27)$$

b) If $a_{i-1} = 0$, then

$$\begin{aligned} k_2 = k_6 = 0, \quad k_1 = \pm k_5 \\ k_4 = k_8 = 0, \quad k_3 = \pm k_7 \end{aligned} \quad (28)$$

Then, we substitute the above equation into equation (21) resulting in the following linear relationship:

$$J_{d_{i-1}} = \pm J_{d_i}$$

$$J_{\theta_{i-1}} = \pm J_{\theta_i} \quad (29)$$

2) MEASURE ONLY THE END POSITION

Because it is difficult to measure the end attitude accurately, when performing the calibration of the robot kinematic parameters, it is common only to measure the end position. Therefore, if the parameter identification is performed only based on the end position, other linearly correlated sub-columns of the Jacobian matrix may exist in the identification model, which is in addition to the linear relationship shown in equations (27) and (29). In which case, only the first three rows of the Jacobian matrix need to be analyzed, resulting in the additional linearly correlated sub-columns of the Jacobian matrix:

1. If $a_N \neq 0$, then

$${}^d J_{\alpha_N} = 0 \quad (30)$$

2. If $a_N = 0$ and $d_N \neq 0$, then

$$\begin{aligned} {}^d J_{\alpha_N} &= 0 \\ {}^d J_{\theta_N} &= 0 \\ {}^d J_{\theta_{N-1}} &= -\frac{a_{N-1} \cos \alpha_{N-1}}{d_N} {}^d J_{\alpha_{N-1}} + d_N \sin \alpha_{N-1} {}^d J_{a_{N-1}} \\ &\quad - a_{N-1} \sin \alpha_{N-1} {}^d J_{d_N} \\ {}^d J_{d_{N-1}} &= -\frac{\sin \alpha_{N-1}}{d_N} {}^d J_{\alpha_{N-1}} + \cos \alpha_{N-1} {}^d J_{d_N} \end{aligned} \quad (31)$$

IV. ANALYSIS OF REDUNDANT DH ERROR PARAMETERS AND THEIR PHYSICAL MEANING

In the previous section, the linearly-correlated columns of Jacobian matrices under different conditions were obtained through theoretical derivation. In kinematic parameter identification, the linearly-correlated sub-columns of Jacobian matrices and the corresponding redundant parameters need to be removed. According to equations (29) and (31):

$$\begin{aligned} &J_{d_{i-1}} \Delta d_{i-1} + J_{d_i} \Delta d_i \\ &= \pm J_{d_i} \Delta d_{i-1} + J_{d_i} \Delta d_i = J_{d_i} \tilde{\Delta d}_i \\ &J_{\theta_{i-1}} \Delta \theta_{i-1} + J_{\theta_i} \Delta \theta_i \\ &= \pm J_{\theta_i} \Delta \theta_{i-1} + J_{\theta_i} \Delta \theta_i = J_{\theta_i} \tilde{\Delta \theta}_i \\ &{}^d J_{\theta_{N-1}} \Delta \theta_{N-1} + {}^d J_{d_{N-1}} \Delta d_{N-1} + {}^d J_{\alpha_{N-1}} \Delta \alpha_{N-1} \\ &\quad + {}^d J_{a_{N-1}} \Delta a_{N-1} + {}^d J_{d_N} \Delta d_N \\ &= {}^d J_{\alpha_{N-1}} \tilde{\Delta \alpha}_{N-1} + {}^d J_{a_{N-1}} \tilde{\Delta a}_{N-1} + {}^d J_{d_N} \tilde{\Delta d}_N \end{aligned} \quad (32)$$

where $\tilde{\Delta d}_i$, $\tilde{\Delta \theta}_i$, $\tilde{\Delta \alpha}_{N-1}$, $\tilde{\Delta a}_{N-1}$ and $\tilde{\Delta d}_N$ are the linear independent parameters obtained after removing the

$$F^i = \begin{bmatrix} \cos \theta_i & \sin \theta_i & 0 & -d_i \sin \theta_i & d_i \cos \theta_i & 0 \\ -\sin \theta_i \cos \alpha_i & \cos \theta_i \cos \alpha_i & \sin \alpha_i & a_i \sin \theta_i \sin \alpha_i - d_i \cos \theta_i \cos \alpha_i & -a_i \cos \theta_i \sin \alpha_i - d_i \sin \theta_i \cos \alpha_i & a_i \cos \alpha_i \\ \sin \theta_i \sin \alpha_i & -\cos \theta_i \sin \alpha_i & \cos \alpha_i & a_i \sin \theta_i \cos \alpha_i + d_i \cos \theta_i \sin \alpha_i & -a_i \cos \theta_i \cos \alpha_i + d_i \sin \theta_i \sin \alpha_i & -a_i \sin \alpha_i \\ 0 & 0 & 0 & \cos \theta_i & \sin \theta_i & 0 \\ 0 & 0 & 0 & -\sin \theta_i \cos \alpha_i & \cos \theta_i \cos \alpha_i & \sin \alpha_i \\ 0 & 0 & 0 & \sin \theta_i \sin \alpha_i & -\cos \theta_i \sin \alpha_i & \cos \alpha_i \end{bmatrix} \quad (14)$$

redundant parameters. The redundant DH error parameters and linear independent parameters of the robots with different identification conditions and different configurations are summarized as follows:

According to Table 1, firstly analyzed are the physical meaning of redundant parameters when measuring the end position and attitude.

If $\alpha_{i-1} \neq 0$ and $\alpha_{i-1} \neq 180^\circ$, the axes of the two adjacent joint rotation axes are therefore not parallel, and there is no redundant parameter at this time.

If $\alpha_{i-1} = 0$ or $\alpha_{i-1} = 180^\circ$, and $a_{i-1} \neq 0$, the robot configurations are shown in Figure 2(a). At this time, the axes of the two adjacent joints are parallel but not collinear. The translation along axis Z_{i-2} , d_{i-1} and the translation along axis Z_{i-1} , d_i have the same or opposite effects on the position and attitude of point P. The current redundant parameter is Δd_{i-1} .

If $\alpha_{i-1} = 0$ or $\alpha_{i-1} = 180^\circ$, and $a_{i-1} = 0$, the robot configurations are shown in Figure 2(b) where the two adjacent joint axes are parallel and collinear. Apart from the correlation between the effects of d_{i-1} and d_i on the position and attitude of Point P, the rotation around axis Z_{i-2} , θ_{i-1} and the rotation around axis Z_{i-1} , θ_i also have the same or opposite effects on the position and attitude of point P. The current redundant parameters are Δd_{i-1} , $\Delta \theta_{i-1}$.

In addition to the parameters of Δd_{i-1} , $\Delta \theta_{i-1}$, there are other redundant parameters in the identification model when only the end position is measured. The specific redundant parameters are closely related to the robot's configurations.

If $a_N \neq 0$, the rotation angle around axis X_N , α_N only affects the attitude of the end point P_e without affecting the end position. The only additional redundant parameter is $\Delta \alpha_N$.

If $a_N = 0$ and $d_N \neq 0$, for the convenience of analysis and explanation, it can be divided into two cases: $\alpha_{N-1} = 0$ and $\alpha_{N-1} = 90^\circ$, as shown in Figures 3 and 4. In addition to ${}^dJ_{\alpha_N} = 0$ and ${}^dJ_{\theta_N} = 0$, when $\alpha_{N-1} = 0$, the linearly correlated sub-columns of the Jacobian matrix has the following relationship at this time:

$$\begin{aligned} {}^dJ_{\theta_{N-1}} &= -\frac{a_{N-1}}{d_N} {}^dJ_{\alpha_{N-1}} \\ {}^dJ_{d_{N-1}} &= {}^dJ_{d_N} \end{aligned} \quad (33)$$

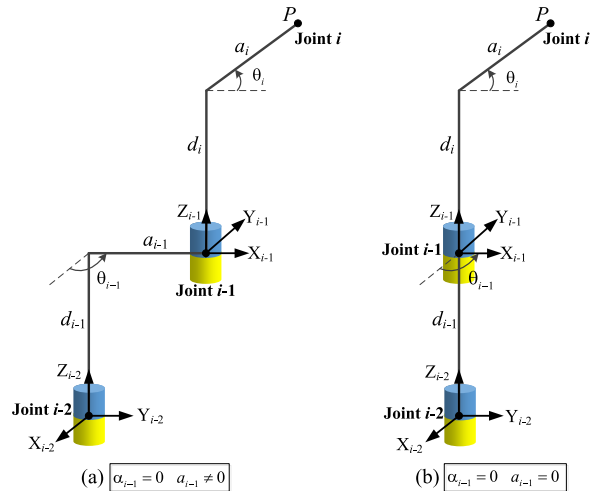


FIGURE 2. Configuration analysis upon the redundant parameters when measuring the end position and attitude.

When $\alpha_{N-1} = 90^\circ$, we have:

$$\begin{aligned} {}^dJ_{\theta_{N-1}} &= d_N {}^dJ_{a_{N-1}} - a_{N-1} {}^dJ_{d_N} \\ {}^dJ_{d_{N-1}} &= -\frac{1}{d_N} {}^dJ_{\alpha_{N-1}} \end{aligned} \quad (34)$$

Figures 3 and 4 show the configuration in which redundant parameters exist when the end position is the only one measured. The influence of different parameter errors on the end position of the robot is described as follows. The dotted line is the robot's configuration when considering the parameter errors. It can be seen that α_N and θ_N do not affect the position of end point regardless of the values of α_{N-1} . Therefore, $\Delta \alpha_N$ and $\Delta \theta_N$ are redundant parameters.

When $\alpha_{N-1} = 0$, the rotation angle error around axis Z_{N-2} , $\Delta \theta_{N-1}$ and axis X_{N-1} , $\Delta \alpha_{N-1}$ have the same effects on the displacement of the robot's end point, as shown in Figure 3(a). The resulting end errors are equal when the parameter errors are $\Delta \alpha_{N-1} = -(a_{N-1}/d_N) \cdot \Delta \theta_{N-1}$. Additionally, the translation error along axis Z_{N-2} , Δd_{N-1} and along axis Z_{N-1} , Δd_N also have the same effects on the end point positions, as shown in Figure 3(b). The end errors are equal when the parameter errors are $\Delta d_N = \Delta d_{N-1}$.

When $\alpha_{N-1} = 90^\circ$, the rotation angle error around axis Z_{N-2} , $\Delta \theta_{N-1}$ have the same effects on the displacement

$$\begin{aligned} k_1(\sin \theta_i a_{i-1} \cos \alpha_{i-1} + d_i \cos \theta_i \sin \alpha_{i-1}) - k_2 d_i \sin \theta_i + k_3 \sin \theta_i \sin \alpha_{i-1} + k_4 \cos \theta_i &= k_8 \\ k_1[\cos \theta_i \cos \alpha_i a_{i-1} \cos \alpha_{i-1} - \sin \alpha_i a_{i-1} \sin \alpha_{i-1} - (a_i \cos \theta_i \sin \alpha_i + d_i \sin \theta_i \cos \alpha_i) \sin \alpha_{i-1} + a_i \cos \alpha_i \cos \alpha_{i-1}] \\ + k_2(a_i \sin \theta_i \sin \alpha_i - d_i \cos \theta_i \cos \alpha_i) + k_3(\cos \theta_i \cos \alpha_i \sin \alpha_{i-1} + \sin \alpha_i \cos \alpha_{i-1}) - k_4 \sin \theta_i \cos \alpha_i &= k_5 a_i \cos \alpha_i + k_7 \sin \alpha_i \\ k_1[-\cos \theta_i \sin \alpha_i a_{i-1} \cos \alpha_{i-1} - \cos \alpha_i a_{i-1} \sin \alpha_{i-1} + (-a_i \cos \theta_i \cos \alpha_i + d_i \sin \theta_i \sin \alpha_i) \sin \alpha_{i-1} - a_i \sin \alpha_i \cos \alpha_{i-1}] \\ + k_2(a_i \sin \theta_i \cos \alpha_i + d_i \cos \theta_i \sin \alpha_i) + k_3(-\cos \theta_i \sin \alpha_i \sin \alpha_{i-1} + \cos \alpha_i \cos \alpha_{i-1}) + k_4 \sin \theta_i \sin \alpha_i &= -k_5 a_i \sin \alpha_i + k_7 \cos \alpha_i \\ k_1 \sin \theta_i \sin \alpha_{i-1} + k_2 \cos \theta_i &= k_6 \\ k_1(\cos \theta_i \cos \alpha_i \sin \alpha_{i-1} + \sin \alpha_i \cos \alpha_{i-1}) - k_2 \sin \theta_i \cos \alpha_i &= k_5 \sin \alpha_i \\ k_1(-\cos \theta_i \sin \alpha_i \sin \alpha_{i-1} + \cos \alpha_i \cos \alpha_{i-1}) + k_2 \sin \theta_i \sin \alpha_i &= k_5 \cos \alpha_i \end{aligned} \quad (23)$$

TABLE 1. Redundant DH error parameters and linear independent parameters ((a) denotes measuring the end pose, (b) denotes measuring only the end position).

Identification conditions	Linearly-correlated columns of Jacobian matrices	Redundant DH error parameters	Linear independent parameters
$\alpha_{i-1} \neq 0$ and $\alpha_{i-1} \neq 180^\circ$	--	--	--
(a) $\alpha_{i-1} = 0$ or $\alpha_{i-1} = 180^\circ$	$\mathbf{J}_{d_{i-1}} = \pm \mathbf{J}_{d_i}$ $\mathbf{J}_{\theta_{i-1}} = \pm \mathbf{J}_{\theta_i}$	Δd_{i-1} Δd_{i-1} $\Delta \theta_{i-1}$	$\Delta \tilde{d}_i = \pm \Delta d_{i-1} + \Delta d_i$ $\Delta \tilde{d}_i = \pm \Delta d_{i-1} + \Delta d_i$ $\Delta \tilde{\theta}_i = \pm \Delta \theta_{i-1} + \Delta \theta_i$
Identification conditions	New added linearly-correlated columns	New added redundant parameters	New added linear independent parameters
$a_N \neq 0$	${}^d \mathbf{J}_{\alpha_N} = 0$	$\Delta \alpha_N$	--
(b) $a_N = 0$ and $d_N \neq 0$	${}^d \mathbf{J}_{\alpha_N} = 0$ ${}^d \mathbf{J}_{\theta_N} = 0$ ${}^d \mathbf{J}_{\theta_{N-1}} = -\frac{a_{N-1} \cos \alpha_{N-1}}{d_N} {}^d \mathbf{J}_{\alpha_{N-1}} + d_N \sin \alpha_{N-1} {}^d \mathbf{J}_{a_{N-1}} - a_{N-1} \sin \alpha_{N-1} {}^d \mathbf{J}_{d_N}$ ${}^d \mathbf{J}_{d_{N-1}} = -\frac{\sin \alpha_{N-1}}{d_N} {}^d \mathbf{J}_{\alpha_{N-1}} + \cos \alpha_{N-1} {}^d \mathbf{J}_{d_N}$	$\Delta \alpha_N$ $\Delta \theta_N$ $\Delta \theta_{N-1}$ Δd_{N-1}	$\Delta \tilde{\alpha}_{N-1} = -\frac{a_{N-1} \cos \alpha_{N-1}}{d_N} \Delta \theta_{N-1}$ $-\frac{\sin \alpha_{N-1}}{d_N} \Delta d_{N-1} + \Delta \alpha_{N-1}$ $\Delta \tilde{d}_{N-1} = d_N \sin \alpha_{N-1} \Delta \theta_{N-1} + \Delta a_{N-1}$ $\Delta \tilde{d}_N = -a_{N-1} \sin \alpha_{N-1} \Delta \theta_{N-1} + \cos \alpha_{N-1} \Delta d_{N-1} + \Delta d_N$

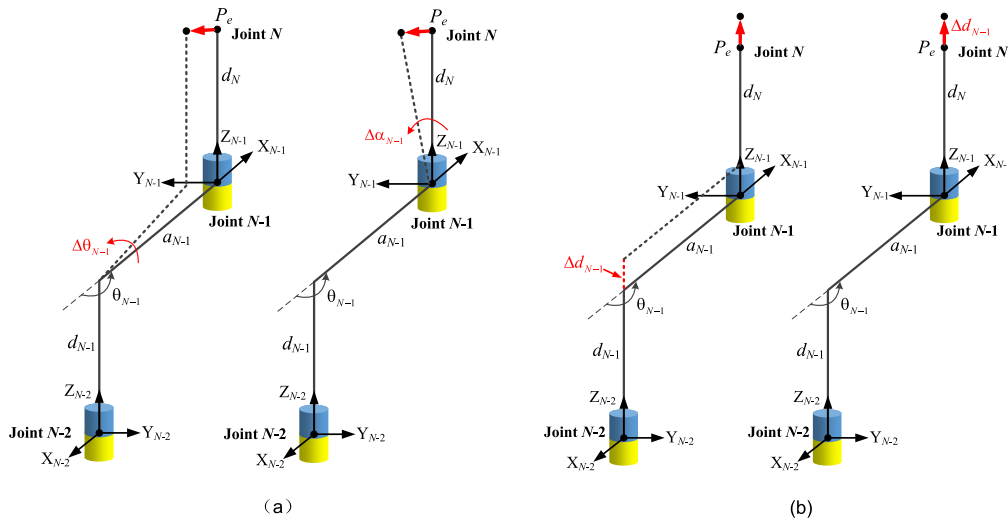


FIGURE 3. Configuration analysis upon the redundant parameters when measuring only the end position ($a_N = 0$ $d_N \neq 0$ $\alpha_{N-1} = 0$). (a) Rotation around axis Z_{N-2} . (b) Translation along axis Z_{N-2} .

of the robot's end point with the combined effects of the translation error along axis X_{N-1} , Δa_{N-1} and along axis Z_{N-1} , Δd_N , as shown in Figure 4(a). The end errors are equal when the parameter errors are $\Delta a_{N-1} = d_N \Delta \theta_{N-1}$

and $\Delta d_N = -a_{N-1} \Delta \theta_{N-1}$. Furthermore, the translation error along axis Z_{N-2} , Δd_{N-1} have the same effects on the displacement of robot end points with the rotation angle error around axis X_{N-1} , Δa_{N-1} , as shown in Figure 4(b).

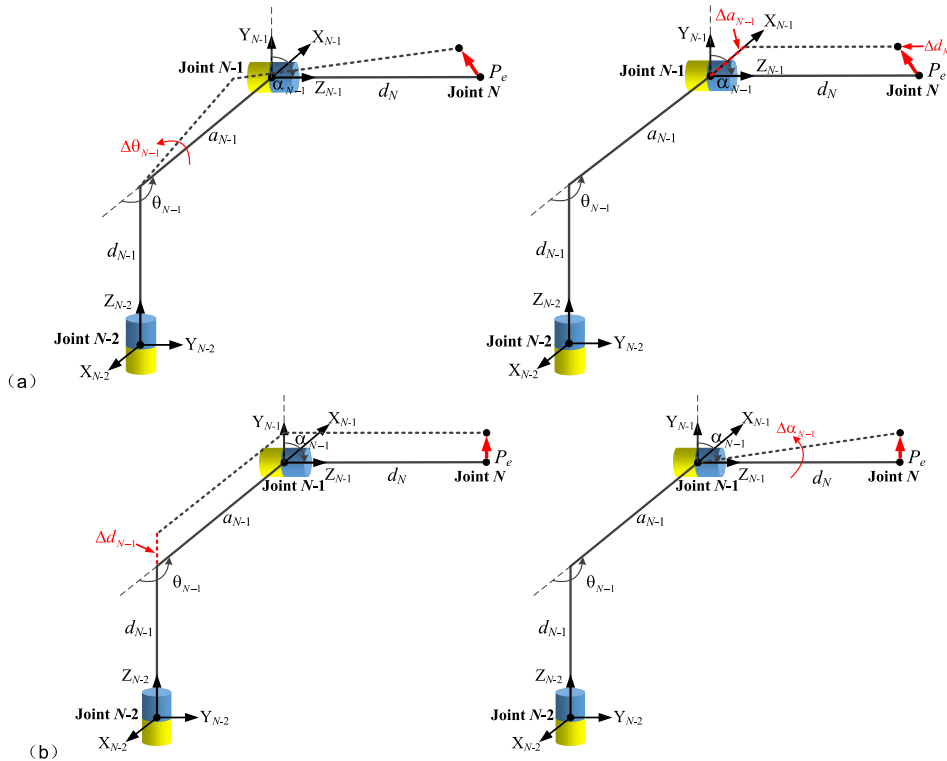


FIGURE 4. Configuration analysis upon the redundant parameters when measuring only the end position ($a_N = 0$ $d_N \neq 0$ $\alpha_{N-1} = 90^\circ$). (a) Rotation around axis Z_{N-2} . (b) Translation along axis Z_{N-2} .

The end errors are equal when the parameter errors are $\Delta\alpha_{N-1} = -\Delta d_{N-1}/d_N$.

V. VERIFICATION OF REDUNDANCY ANALYSIS RESULTS THROUGH SIMULATION EXPERIMENT

Because it is usually difficult to measure the exact values of the robot end attitude in the experiment, this paper only uses the end position error to identify the kinematic parameters. To solve all the unknown parameters, multiple sets of end position data and corresponding joint angle data need to be measured. Assuming there are r groups of end position data and joint angle data, the kinematic parameter identification model at this time is

$$\begin{bmatrix} {}^E d(q_1) \\ {}^E d(q_2) \\ \vdots \\ {}^E d(q_r) \end{bmatrix} = \begin{bmatrix} {}^d J(q_1) \\ {}^d J(q_2) \\ \vdots \\ {}^d J(q_r) \end{bmatrix} \Delta X \quad (35)$$

According to the linear equation group in the above equation, the least square method is used to identify the kinematic parameter error ΔX . Accordingly, the kinematic parameters of the robot can be calibrated.

The least square method for error parameters identification is given below. Equation (35) can be written in the following form:

$$d = Jx \quad (36)$$

where $d = {}^E d \in \mathbf{R}^m$, $J = {}^d J \in \mathbf{R}^{m \times n}$, $x = \Delta X \in \mathbf{R}^n$, and $m = 3r$, $n = 4N$. Calculating x so that equation $\|d - Jx\|_2$ reaches the minimum value. At this time, x is called the least square solution of equation (36).

Since the number of rows m of matrix J is greater than the number of columns n , J is not a row-full-rank matrix. Therefore, the generalized inverse of matrix is introduced to give the general solution of the least square method.

Suppose there is a matrix $B \in \mathbf{R}^{n \times m}$ that satisfies:

$$\begin{aligned} JBJ &= J, & BJB &= B \\ (JB)^T &= JB, & (BJ)^T &= BJ \end{aligned} \quad (37)$$

then B is called the generalized inverse of matrix J , denoted as J^+ .

The general solution of x can be written as

$$x = J^+d + (I_n - J^+J)z \quad (38)$$

where z is an arbitrary n -dimensional vector. Among these general solutions, when $x = J^+d$, $\|d - Jx\|_2$ reaches the minimum value ($\min_{x=J^+d} \|d - Jx\|_2 = \|(I_m - JJ^+)d\|_2$), which means $x = J^+d$ is the least square solution.

A. KINEMATIC PARAMETER IDENTIFICATION SIMULATION EXPERIMENT OF ROBOTS

The experiment object in this paper is a robot with six rotating joints. Figure 5 is the schematic diagram of the robot joint

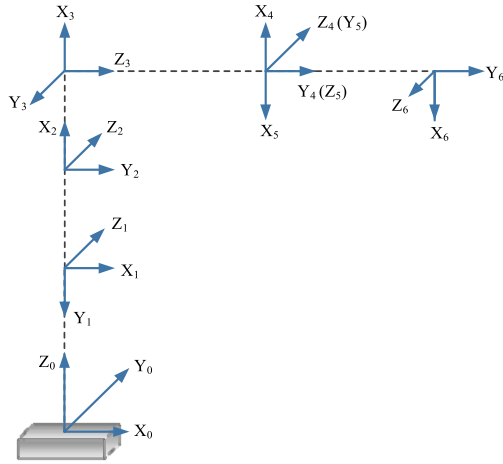


FIGURE 5. Robot joint coordinate system.

TABLE 2. DH parameter nominal values and angle range of joint motion.

<i>i</i>	Angle range of joint motion (deg)	d_i / mm	θ_i / deg	a_i / mm	α_i / deg
1	-180, 180	615	0	0	-90
2	-100, 110	0	-90	705	0
3	-60, 60	0	0	135	-90
4	-180, 180	755	0	0	90
5	-120, 120	0	180	0	90
6	-180, 180	85	0	0	90

coordinate system. Table 2 shows the nominal values of the DH parameters and the angle range of joint motion.

According to the nominal values of the DH parameters shown in Table 2, we obtain $\alpha_2 = 0, a_2 = 705 \neq 0, a_6 = 0, d_6 = 85 \neq 0,$ and $a_5 = 0, \alpha_5 = 90^\circ$. Therefore, according to Table 1, the following linearly-correlated sub-columns of the Jacobian matrix can be obtained:

$$\begin{aligned}
 \mathbf{J}_{d_2} &= \mathbf{J}_{d_3} \\
 {}^d\mathbf{J}_{\alpha_6} &= \mathbf{0} \\
 {}^d\mathbf{J}_{\theta_6} &= \mathbf{0} \\
 {}^d\mathbf{J}_{\theta_5} &= d_6 {}^d\mathbf{J}_{a_5} \\
 {}^d\mathbf{J}_{d_5} &= -\frac{1}{d_6} {}^d\mathbf{J}_{\alpha_5}
 \end{aligned} \tag{39}$$

According to the above equation, the six-degree-of-freedom robot shown in Figure 5 has five redundant DH error parameters. It should be noted that the linearly correlated parameters have equivalent effect on the end position and attitude, so it is ok to remove any parameter from the correlated parameters, and the effect on the end position and attitude can be characterized by the retained parameters. In this paper, $\Delta d_2, \Delta \alpha_6, \Delta \theta_6, \Delta \theta_5$ and Δd_5 are selected as redundant parameters. Before parameter identification, all redundant parameters need to be removed, and the corresponding columns of the identification Jacobian matrix are

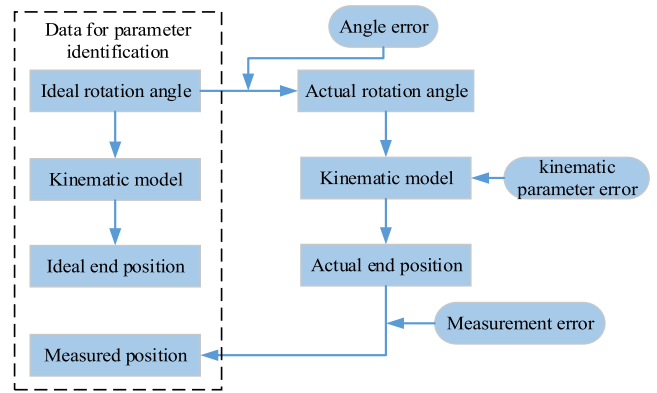


FIGURE 6. Flow chart of simulation experiment.

removed to form a new Jacobian matrix (${}^d\tilde{\mathbf{J}}$). At this point, the kinematic parameter identification model becomes

$${}^d\tilde{\mathbf{J}}\Delta\tilde{\mathbf{X}} = \mathbf{E}d \tag{40}$$

In the above equation, $\Delta\tilde{\mathbf{X}} = [\Delta d \ \Delta\theta \ \Delta a \ \Delta\alpha]^T$ are the kinematic error parameters to be identified. After removing the redundant parameter, the unknown parameter to be identified is reduced from 24 to 19, and each component is shown as follows:

$$\begin{aligned}
 \Delta d &= [\Delta d_1 \ \Delta\tilde{d}_3 \ \Delta d_4 \ \Delta d_6] \\
 \Delta\theta &= [\Delta\theta_1 \ \Delta\theta_2 \ \Delta\theta_3 \ \Delta\theta_4] \\
 \Delta a &= [\Delta a_1 \ \Delta a_2 \ \Delta a_3 \ \Delta a_4 \ \Delta\tilde{a}_5 \ \Delta a_6] \\
 \Delta\alpha &= [\Delta\alpha_1 \ \Delta\alpha_2 \ \Delta\alpha_3 \ \Delta\alpha_4 \ \Delta\tilde{\alpha}_5]
 \end{aligned} \tag{41}$$

In the above equation, $\Delta\tilde{d}_3, \Delta\tilde{a}_5, \Delta\tilde{\alpha}_5$ are the linearly-independent parameters obtained after removing the redundant parameters; the originally identified $\Delta d_3, \Delta a_5, \Delta\alpha_5$ become a linear combination of several other parameters, according to Table 1.

$$\begin{aligned}
 \Delta\tilde{d}_3 &= \Delta d_2 + \Delta d_3 \\
 \Delta\tilde{a}_5 &= d_6\Delta\theta_5 + \Delta a_5 \\
 \Delta\tilde{\alpha}_5 &= -\frac{1}{d_6}\Delta d_5 + \Delta\alpha_5
 \end{aligned} \tag{42}$$

To perform the kinematic parameter identification simulation experiment, it is necessary to first set the kinematic parameter error to generate the identification data. Then, multiple sets of joint rotation angles are generated within the angle range of robot joint motion. According to the kinematic model and kinematic parameter error, the ideal end position and actual end position of the robot are obtained. To consider the random noise caused by driving the joint and end measurement, it is also necessary to introduce the joint angle error and end measurement error to generate the robot end position measurement value. Finally, the kinematic parameter error is identified according to the ideal rotation angle, kinematic model, and measurement position, as shown in Figure 6.

The following section analyzes and compares the full parameter identification and non-redundant parameter identification results without noise and with random noise, which

TABLE 3. True values of DH parameter error.

i	$\Delta d_i^R / \text{mm}$	$\Delta \theta_i^R / \text{deg}$	$\Delta a_i^R / \text{mm}$	$\Delta \alpha_i^R / \text{deg}$
1	0.50	0.07	0.22	0.08
2	0.15	0.12	0.35	0.05
3	0.47	0.11	0.52	0.02
4	1.10	0.09	0.45	0.05
5	0.24	0.04	0.54	0.11
6	0.32	0.10	0.05	0.1

verify the analysis results of parameter redundancy summarized in Table 1. This section also analyzes the impact of removing redundant parameters on the effectiveness of identification.

B. WITHOUT RANDOM NOISE

To better verify the correctness of the parameter redundancy analysis, the simulation experiments in this section do not consider random noise, such as joint rotation angle error and end measurement error. Table 3 gives the true values of the DH parameter errors ($\Delta d_i^R, \Delta \theta_i^R, \Delta a_i^R, \Delta \alpha_i^R$). Then, 60 sets of sampling data points are selected within the angle range of joint motion. Based on these data, the kinematic parameters are identified by the full parameter model (equation (35)) and the non-redundant parameter model (equation (37)), respectively.

Table 4 gives the full parameter identification results ($\Delta d_i^F, \Delta \theta_i^F, \Delta a_i^F, \Delta \alpha_i^F$) and non-redundant parameter identification results ($\Delta d_i^{N-R}, \Delta \theta_i^{N-R}, \Delta a_i^{N-R}, \Delta \alpha_i^{N-R}$). As evidenced by the data in Table 4, when using full parameter identification, the eight parameters in the box (i.e., $\Delta d_2, \Delta d_3, \Delta d_5, \Delta \theta_5, \Delta \theta_6, \Delta a_5, \Delta \alpha_5, \Delta \alpha_6$) are not accurately identified, whereas other parameter identification results are accurate. When using non-redundant parameter identification, only $\Delta d_3, \Delta a_5, \Delta \alpha_5$ are quite different from the set of true values. Equation (39) indicates that, after removing the redundant parameters, these three parameters become a linear combination of several other parameters. According to the calculation, $\Delta \tilde{d}_3 = 0.62, \Delta \tilde{a}_5 = 0.599, \Delta \tilde{\alpha}_5 = -0.052$, which are very close to the identification results. Therefore, after removing the redundant parameters, the DH error parameters are accurately identified. By analyzing the Jacobian matrix, the ranks of the Jacobian matrices of the full-parameter model and the non-redundancy model are 19, that is $R(d^d J) = R(d^{\tilde{d}} J) = 19 < 24$. Therefore, there are indeed five redundant parameters in the full-parameter model, so not all the DH parameters can be identified. Moreover, the five parameters removed from the non-redundant parameter model are all redundant parameters, which further verifies the correctness of the parameter redundancy analysis results.

According to the identification results in Table 4, the DH parameters are corrected. Then, 60 sets of joint angles are randomly selected to verify the calibration effects on the robot

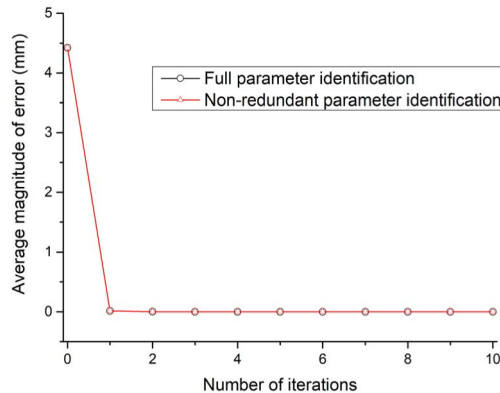


FIGURE 7. Endpoint errors after different number of iterations (without random noise).

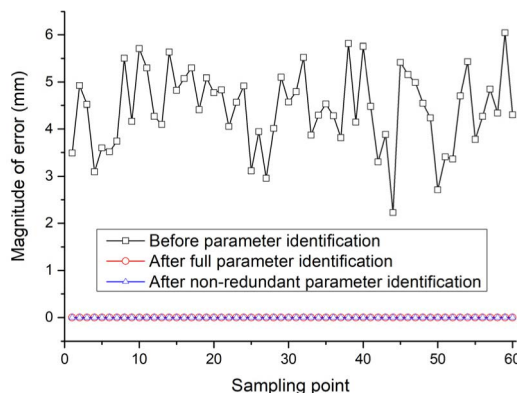


FIGURE 8. Magnitude of errors at sampling points.

end errors without random noise. Figure 7 and Figure 8 show the variation of the end error average value with the number of iterations and the amount of the end error at each sampling point. The figure indicates that, regardless of whether the full parameter identification or the non-redundant parameter identification is used, the end error quickly converges when the number of iterations is increased, indicating that when the random noise is not considered—even though the full-parameter identification cannot accurately identify all the kinematic parameters—it still has a good optimization effect on the robot end accuracy.

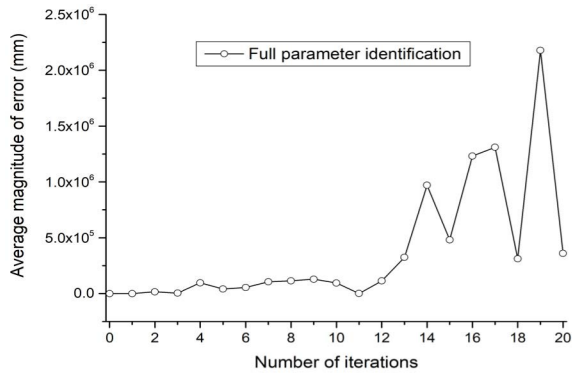
C. CONSIDER RANDOM NOISE

In the actual experiment, random noise is unavoidable. When considering the random noise, the existence of redundant parameters will impact the accuracy and stability of identification. Therefore, this section considers the random noise introduced by driving the joint and end measurements. Assume the variation range of joint angle errors and end position measurement errors are $[-0.0001, 0.0001](\text{rad})$ and $[-0.3, 0.3](\text{mm})$ respectively.

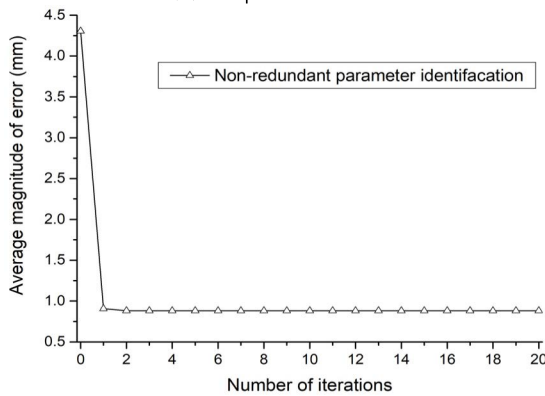
The full parameter identification and the non-redundant parameter identification are respectively performed to obtain the variations of the calibrated end position errors with the number of iterations, as shown in Figure 9. The figure shows

TABLE 4. Parameter identification results without random noise.

i	$\Delta d_i^F / \text{mm}$	$\Delta d_i^{N-R} / \text{mm}$	$\Delta \theta_i^F / \text{deg}$	$\Delta \theta_i^{N-R} / \text{deg}$	$\Delta a_i^F / \text{mm}$	$\Delta a_i^{N-R} / \text{mm}$	$\Delta \alpha_i^F / \text{deg}$	$\Delta \alpha_i^{N-R} / \text{deg}$
1	0.5020	0.5020	0.0700	0.0700	0.2153	0.2153	0.0800	0.0800
2	0.3152	--	0.1197	0.1197	0.3524	0.3524	0.0510	0.0510
3	0.3152	0.6304	0.1134	0.1134	0.5521	0.5521	0.0182	0.0182
4	1.0868	1.0868	0.0913	0.0913	0.4508	0.4508	0.0558	0.0558
5	0	--	0.4027	--	0.0001	0.5975	-0.0534	-0.0534
6	0.3253	0.3253	0	--	0.0492	0.0492	0	--



(a) Full parameter identification



(b) Non-redundant parameter identification

FIGURE 9. Endpoint errors after different number of iterations (consider random noise).

that, in the case of non-redundant parameter identification, when the number of iterations increases, the calibrated end position error decreases rapidly and converges. The average error is reduced from 4.31 mm to 0.88 mm. However, with full parameter identification, the calibrated end position error is not reduced, but it gradually increases with the number of iterations. When considering the noise, if there are redundant parameters in the identification model, the parameter identification result is difficult to converge, and the effect of calibrating the end error cannot be achieved. If the redundant parameters in the identification model are eliminated, the stability of the identification can be improved, and the end position error can still be reduced in the presence of noise.

TABLE 5. Non-redundant parameter identification results with the presence of random noise.

i	$\Delta d_i^{N-R} / \text{mm}$	$\Delta \theta_i^{N-R} / \text{deg}$	$\Delta a_i^{N-R} / \text{mm}$	$\Delta \alpha_i^{N-R} / \text{deg}$
1	0.5587	0.0500	0.1210	0.0889
2	--	0.0964	1.1646	0.0968
3	0.5345	0.1819	0.3077	-0.0199
4	1.1655	0.1251	0.1633	0.2136
5	--	--	0.1152	-0.1853
6	0.5754	--	0.1194	--

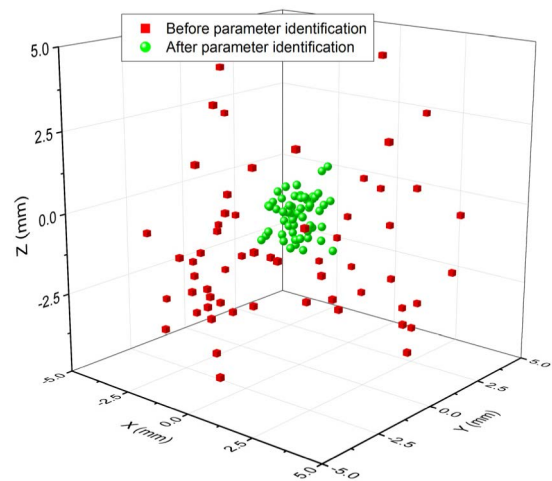


FIGURE 10. Spatial distribution of errors before and after parameter identification.

Table 5 gives the identification results without redundant parameters. Comparing these results with the DH parameter errors shown in Table 3, it seems that, with the presence of random noise, many of the identification results are close to the set values. Therefore, the calibrated end position error is still greatly reduced, even though it is not close to zero. Figure 10 shows the spatial distribution of the end position error of each sampling point. Visually, the end error before calibration is roughly distributed within the interval of $[-5, 5](\text{mm})$, which falls in the interval of $[-1.2, 1.2](\text{mm})$ after calibration. So, the spatial distribution range of the end error is significantly reduced after calibration. According to the above analysis, because the noise in the robot parameter calibration experiment is unavoidable, the redundant

parameters in the identification model must be eliminated for the accurate kinematic parameter identification, thereby improving the end accuracy of the robot.

VI. CONCLUSION

This paper systematically analyzes the redundant parameters of robots under various identification conditions and based on the DH parameter error model. The coupling relation of the linear dependent columns of the identification Jacobian matrix is derived analytically. Traditionally, it is determined by the numerical analysis. Thus, the proposed method could facilitate the determination of the non-redundant kinematic calibration model. Table 1 provides the redundant DH error parameters of the robot in different identification conditions and with different geometric configurations. Figures 2–4 illustrate the physical meaning of the redundant parameters. According to the parameter redundancy analysis results, we can quickly determine the redundant parameters of robots with different configurations and thus perform the non-redundant parameter identification.

To verify and analyze the results of parameter redundancy analysis, a six-degree-of-freedom robot was taken as an example to carry out the parameter identification simulation experiment. According to the theoretical analysis results in Table 1, the robot has five redundant parameters. After removing the redundant parameters, the kinematic parameters are all accurately identified without considering random noise. The calibrated end position error approaches zero, which fully verifies the correctness of the parameter redundancy analysis results. When considering random noise, due to the existence of redundant parameters, the full parameter identification results are difficult to converge, and the end position error is not reduced but increased. After removing the redundant parameters, the identification results have good convergence.

This paper presents an analytical method to determine the redundant parameters of robots. At present, the research of this paper is in the stage of theoretical analysis and simulation experiment, which needs further experimental verification in the future work. In addition, the analysis method can be extended to other kinematic models for non-redundant parameter identification of robots.

REFERENCES

- [1] P. S. Shiakolas, K. L. Conrad, and T. C. Yih, "On the accuracy, repeatability, and degree of influence of kinematics parameters for industrial robots," *Int. J. Model. Simul.*, vol. 22, no. 4, pp. 245–254, Jan. 2002.
- [2] A. Nubiola and I. A. Bonev, "Absolute robot calibration with a single telescoping ballbar," *Precis. Eng.*, vol. 38, no. 3, pp. 472–480, Jul. 2014.
- [3] A. Nubiola and I. A. Bonev, "Absolute calibration of an ABB IRB 1600 robot using a laser tracker," *Robot. Comput.-Integr. Manuf.*, vol. 29, no. 1, pp. 236–245, Feb. 2013.
- [4] W.-L. Li, H. Xie, G. Zhang, S.-J. Yan, and Z.-P. Yin, "Hand-eye calibration in visually-guided robot grinding," *IEEE Trans. Cybern.*, vol. 46, no. 11, pp. 2634–2642, Nov. 2016.
- [5] J. Wang, W. Wang, C.-H. Wu, S.-L. Chen, J.-H. Fu, and G.-D. Lu, "A plane projection based method for base frame calibration of cooperative manipulators," *IEEE Trans. Ind. Informat.*, vol. 15, no. 3, pp. 1688–1697, Mar. 2018.
- [6] X.-L. Zhong, J. M. Lewis, and F. L. N. Nagy, "Autonomous robot calibration using a trigger probe," *Robot. Auto. Syst.*, vol. 18, no. 4, pp. 395–410, Oct. 1996.
- [7] M. A. Meggiolaro, S. Dubowsky, and C. Mavroidis, "Geometric and elastic error calibration of a high accuracy patient positioning system," *Mech. Mach. Theory*, vol. 40, no. 4, pp. 415–427, Apr. 2005.
- [8] A. Klimchik, B. Furet, S. Caro, and A. Pashkevich, "Identification of the manipulator stiffness model parameters in industrial environment," *Mech. Mach. Theory*, vol. 90, pp. 1–22, Aug. 2015.
- [9] J. M. Hollerbach and C. W. Wampler, "The calibration index and taxonomy for robot kinematic calibration methods," *Int. J. Robot. Res.*, vol. 15, no. 6, pp. 573–591, Dec. 1996.
- [10] K. Schröer, S. L. Albright, and M. Grethlein, "Complete, minimal and model-continuous kinematic models for robot calibration," *Robot. Comput.-Integr. Manuf.*, vol. 13, no. 1, pp. 73–85, Mar. 1997.
- [11] R. He, Y. Zhao, S. Yang, and S. Yang, "Kinematic-parameter identification for serial-robot calibration based on POE formula," *IEEE Trans. Robot.*, vol. 26, no. 3, pp. 411–423, Jun. 2010.
- [12] F. W. Yin, W. J. Tian, H. T. Liu, T. Huang, and D. G. Chetwynd, "A screw theory based approach to determining the identifiable parameters for calibration of parallel manipulators," *Mech. Mach. Theory*, vol. 145, Mar. 2020, Art. no. 103665.
- [13] J. Denavit and R. S. Hartenberg, "A kinematic notation for lower-pair mechanisms based on matrices," *J. Appl. Mech.*, vol. 22, no. 2, pp. 215–221, Jun. 1955.
- [14] W. K. Veitschegger and C.-H. Wu, "Robot calibration and compensation," *IEEE J. Robot. Autom.*, vol. 4, no. 6, pp. 643–656, Dec. 1988.
- [15] P. I. Corke, "A simple and systematic approach to assigning Denavit–Hartenberg parameters," *IEEE Trans. Robot.*, vol. 23, no. 3, pp. 590–594, Jun. 2007.
- [16] E. Dean-Leon, S. Nair, and A. Knoll, "User friendly MATLAB-toolbox for symbolic robot dynamic modeling used for control design," in *Proc. IEEE Int. Conf. Robot. Biomimetics (ROBIO)*, Dec. 2012, pp. 2181–2188.
- [17] A. Dasari and N. S. Reddy, "Forward and inverse kinematics of a robotic frog," in *Proc. 4th Int. Conf. Intell. Hum. Comput. Interact. (IHCI)*, Dec. 2012, pp. 1–5.
- [18] H. Zhuang, Z. S. Roth, and F. Hamano, "A complete and parametrically continuous kinematic model for robot manipulators," *IEEE Trans. Robot. Autom.*, vol. 8, no. 4, pp. 451–463, Aug. 1992.
- [19] H. Zhuang and Z. S. Roth, "A linear solution to the kinematic parameter identification of robot manipulators," *IEEE Trans. Robot. Autom.*, vol. 9, no. 2, pp. 174–185, Apr. 1993.
- [20] H. Stone, A. Sanderson, and C. Neuman, "Arm signature identification," in *Proc. IEEE Int. Conf. Robot. Autom.*, Apr. 1986, pp. 41–48.
- [21] H. Stone and A. Sanderson, "A prototype arm signature identification system," in *Proc. IEEE Int. Conf. Robot. Autom.*, Mar. 1987, pp. 175–182.
- [22] H. W. Stone, *Kinematic Modeling, Identification, and Control of Robotic Manipulators*, vol. 29. Springer, 2012.
- [23] K. C. Gupta, "Kinematic analysis of manipulators using the zero reference position description," *Int. J. Robot. Res.*, vol. 5, no. 2, pp. 5–13, Jun. 1986.
- [24] F. C. Park and K. Okamura, "Kinematic calibration and the product of exponentials formula," in *Advances in Robot Kinematics and Computational Geometry*. Springer, 1994, pp. 119–128.
- [25] L. J. Everett and T.-W. Hsu, "The theory of kinematic parameter identification for industrial robots," *J. Dyn. Syst., Meas., Control*, vol. 110, no. 1, pp. 96–100, Mar. 1988.
- [26] L. J. Everett and A. H. Suryhadiprojo, "A study of kinematic models for forward calibration of manipulators," in *Proc. IEEE Int. Conf. Robot. Autom.*, Apr. 1988, pp. 798–800.
- [27] G. Chen, T. Li, M. Chu, Q. X. Jia, and H. X. Sun, "Review on kinematics calibration technology of serial robots," *Int. J. Precis. Eng. Manuf.*, vol. 15, no. 8, pp. 1759–1774, Aug. 2014.
- [28] M. A. Meggiolaro and S. Dubowsky, "An analytical method to eliminate the redundant parameters in robot calibration," in *Proc. Millennium Conf. IEEE Int. Conf. Robot. Automat. Symposia (ICRA)*, Apr. 2000, pp. 3609–3615.
- [29] G. Chen, H. Wang, and Z. Lin, "Determination of the identifiable parameters in robot calibration based on the POE formula," *IEEE Trans. Robot.*, vol. 30, no. 5, pp. 1066–1077, Oct. 2014.
- [30] G. Chen, L. Kong, Q. Li, H. Wang, and Z. Lin, "Complete, minimal and continuous error models for the kinematic calibration of parallel manipulators based on POE formula," *Mech. Mach. Theory*, vol. 121, pp. 844–856, Mar. 2018.

- [31] X. He, Y. Cheng, and Z. Huang, "Transformation of homogeneous coordinates and its application in the analysis of spatial mechanism," *J. Beijing Univ. Chem. Technol.*, vol. 1, pp. 43–46, Mar. 1999.
- [32] B. Mooring, M. Driels, and Z. Roth, *Fundamentals of Manipulator Calibration*. Hoboken, NJ, USA: Wiley, 1991.
- [33] A. Joubair and I. A. Bonev, "Comparison of the efficiency of five observability indices for robot calibration," *Mech. Mach. Theory*, vol. 70, pp. 254–265, Dec. 2013.
- [34] K. Stepanova, T. Pajdla, and M. Hoffmann, "Robot self-calibration using multiple kinematic chains—A simulation study on the iCub humanoid robot," *IEEE Robot. Autom. Lett.*, vol. 4, no. 2, pp. 1900–1907, Apr. 2019.



YUE ZHANG received the B.S. degree in space science and technology, the M.S. degree in man-machine and environmental engineering, and the Ph.D. degree in aeronautical and astronautical science and technology from the Harbin Institute of Technology, Harbin, Heilongjiang, China, in 2011, 2013, and 2018, respectively.

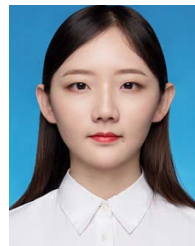
From 2018 to 2022, he was a Lecturer with Xidian University, Xi'an, Shanxi, China. He is the author of more than ten articles. His research

interests include kinematics and dynamics parameter identification of robot/manipulator, and dynamics of multibody systems.



JIAWEN GUO received the B.S. degree in aircraft design engineering and the M.S. degree in man-machine and environmental engineering from the Harbin Institute of Technology, Harbin, Heilongjiang, China, in 2014 and 2016, respectively, where she is currently pursuing the Ph.D. degree in aeronautical and astronautical science and technology.

Her research interests include kinematics and dynamics of multibody systems.



XUEYAN LI received the B.S. degree in automation from the Civil Aviation University of China, in 2020. She is currently pursuing the M.S. degree in mechanical engineering with Xidian University, Xi'an, Shanxi, China.

Her research interests include the dynamics of parallel robots and identification of robot kinematics parameters.

...